Passive compensation of the temperature effect on permanent magnet thrust bearing in hybrid system

Maxence Van Beneden, Virginie Kluyskens, Bruno Dehez

Center for Research in Mechatronics (CEREM), Institute of Mechanics, Materials and Civil Engineering (IMMC),
Université catholique de Louvain (UCL), Louvain-la-Neuve 1348, Belgium
maxence.vanbeneden@uclouvain.be

***Abstract*—Combining a permanent magnet thrust bearing (PMTB) with mechanical bearings inside a hybrid system can be a good compromise for some applications subject to high axial load. The guidance of the shaft is ensured by the mechanical bearings while those latter are relieved from the axial load by the magnetic bearing. However, as the permanent magnet properties depend on the temperature, this load relieve depends on the operating conditions. This paper describes a compensation system to maintain the force developed by the PMTB constant and independent from the temperature. This system consists in a soft spring placed in series with the static part of the PMTB allowing a variation of the airgap thickness. It is shown that when the stiffness of the soft spring is low enough compared to the equivalent stiffness of the PMTB, it is possible to maintain a constant load relieve for a wide range of operating temperature conditions. Practical implementations based on pressurized bellows are described.**

I. INTRODUCTION

Permanent magnet (PM) thrust bearings (PMTB) are compact systems able to generate high axial forces. They are stable in the axial direction but unstable in the radial direction. Combining mechanical bearing (MB) with magnetic bearings in applications subject to high load increases the life time and reduces the losses of the global system [1]. The function of the MB is to locate the shaft. The function of PMTB is to bear the high axial force of the system. Its contribution to guidance and to stabilizing or destabilizing aspects is insignificant, as its stiffness is much lower than the MB stiffness.

This hybrid system can be used in applications with high axial load e.g. flywheel system [2] or turbine [3]. Due to internal losses inside those systems, the operating temperature of PMTB can reach values impacting the load capacity. Indeed, the characteristics of PM material depend on their temperature. A compensation system of the temperature effect based on a soft spring in series with PMTB is described in this article. This compensation system could also act if the PM material properties deteriorate when aging.

This paper presents the model of the soft spring placed in series with the PMTB, analyses their behavior, and describes a practical implementation of the system. First, the complete hybrid system of MB and PMTB compensated by the soft spring is described in section 2. The axial force generated by the PMTB is evaluated by a finite element model depicted in section 3. In section 4, the influence of the soft spring is modeled by an equivalent linearized stiffness model. The impact of the soft spring on the global system is discussed in section 5. Different practical implementations based on pressurized bellows are detailed/given in section 6.

II. SYSTEM DESCRIPTION

The hybrid system is constituted of mechanical bearings (MB) and a permanent magnet thrust bearing (PMTB) as shown in Fig. 1. The total axial load F_{tot} is supposed to be static. The PMTB does not carry the total axial load as a preload has to be maintained on the MB for good operation:

$$F_{tot} = \overbrace{F_{PM}}^{\alpha F_{tot}} + \overbrace{F_{MB}}^{(1-\alpha)F_{tot}} = \text{cst} \quad (1)$$

with F_{PM} and F_{MB} the axial force developed by the PMTB and the MB respectively and $0 \leq \alpha \leq 1$ the coefficient of repartition of the axial load.

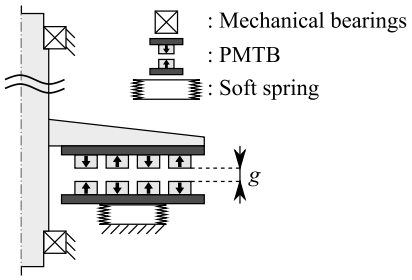

Figure 1. Hybrid system with mechanical bearings and PM thrust bearing. A soft spring is placed in series with the PMTB to compensate the impact of aging and temperature effect on PM material by passively acting on the airgap thickness g.

Because of temperature variation or magnet aging, the characteristics of the PM material may degrade andthe force developped by the PMTB drop. To compensate these effects, the idea is to place an additional soft spring in series with the static part of the PMTB (see Fig. 1). The aim of this spring is to allow an axial displacement of the static part of the PMTB so as to adaptpassively the airgap tickness and maintain a quasi-constant axial force F_{PM}.

III. AXIAL FORCE IN THE PMTB

The axial force developed by the PMTB is obtained by a 2D axisymmetric finite element model (FEM) [4]. The reversible and irreversible demagnetization curves of the PM material are taken into consideration. The force is dependent on the

temperature T and the airgap thickness g. The PM properties and PMTB dimensions are summarized in Table I. These dimensions are obtained from scaling laws minimizing the PM volume [5] considering an axial load $F_{PM} = 20\ kN$, an airgap thickness $g = 3\ mm$ and a remanence $B_r = 1.20\ T$. The PM materiel grade is N35UH and corresponds to the $1.2\ T$ remanence at a temperature of $T_{ref} = 20°C$.

TABLE I. DIMENSIONS AND PROPERTIES OF THE PM RINGS (N35UH)

	Parameters	Value
w	PM width	6.39 mm
h	PM height	2.22 mm
ζ	Space between the rings	2.01 mm
R_{int}	Internal radius	186.3 mm
N	Number of rings	20
$B_{r,20°C}$	Remanence	1.20 T
$H_{k,20°C}$	Coercivity: knee point	1920 kA/m
$H_{cJ,20°C}$	Polarization coercivity	2000 kA/m
$\mu_{r_{PM}}$	PM relative permeability	1.05
α_{B_r}	Temperature coefficient of remanence	-0.11 %/K
α_H	Temperature coefficient of coercivity	-0.5 %/K

The evolution of the axial force with the temperature T for different airgap thicknesses obtained by the FEM are given in Fig. 2. The solid line correponds to the demagnetization curve with reversible (before the knee point of the B-H characteristic) and irreversible effect (after the knee point of the B-H characteristic). The dashed line, extending the first part of the solid line, corresponds to the axial force predicted by the FE model when only reversible demagnetization is considered. Consequently, before the separation point, the demagnetization is reversible. The horizontal line at $F_z = 20\ kN$ corresponds to the reference load. To maintain a constant axial force when the temperature is increased, the airgap thickness has to decrease. To avoid irreversible demagnetization, the temperature may not exceed the maximal temperature $T_{max} = 152\ °C$ for an airgap thickness of $g = 2.2\ mm$.

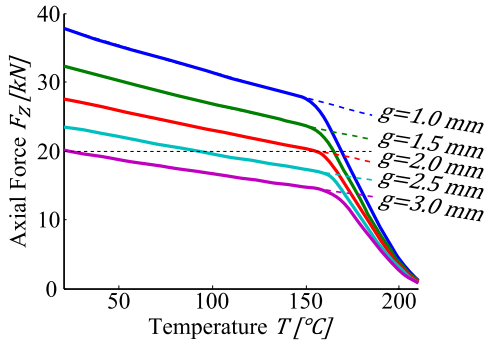

Figure 2. FEM results of the evolution of the axial force with the temperature for different airgap thicknesses. The solid line corresponds to demagnetazation with reversible and irreversible effect and the dashed with only reversible demagnetization.

IV. EQUIVALENT LINEARIZED STIFFNESS MODEL

The axial behavior of the complete hybrid system, including the MB, the PMTB and the soft spring, can be modelled by an equivalent linearized stiffness model as shown in Fig. 3, with k_i the equivalent stiffness and $z_{0,i}$ the equivalent natural length of spring i. The axial positions of the MB, PMTB and soft spring are given by the axial positions of the points (z_1, z_2) and depend on the temperature. The variation of the airgap thickness Δg is equal to the difference of variation of the axial positions of points z_1 and z_2:

$$\Delta g = \Delta z_1 - \Delta z_2 \tag{2}$$

The hypotheses of the equivalent model are that:

- the weight of the soft spring and PMTB are negligible compared to the axial force;
- the soft spring and the MB have a linear behavior with the axial displacement and are independent of the temperature.

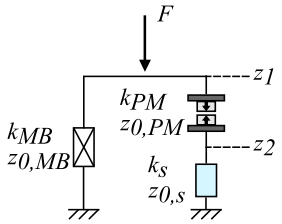

Figure 3. Linearized equivalent stiffness model of the mechanical bearing $(k_{MB},\ z_{0,MB})$, the PMTB $(k_{PM},\ z_{0,PM})$ and the soft spring $(k_s,\ z_{0,s})$ with k_i the equivalent stiffness and $z_{0,i}$ the equivalent naturel length for each element.

The axial force of the PMTB is non-linear with the airgap thickness and the temperature. The linearized model gives the axial force F'_{PM} variation with the airgap thickness g at a given temperature T:

$$F'_{PM}(g,T) = -k_{PM}(g,T)\left(g - z_{0,PM}(g,T)\right) \tag{3}$$

with the equivalent stiffness $k_{PM}(g,T)$ and equivalent natural length $z_{0,PM}(g,T)$ depending on the airgap thickness and the temperature. Figure 4 shows the evolution of the axial force with the airgap thickness for 2 different couples of temperature and airgap thickness $(T = 20°C, g = 3\ mm)$ and $(T = 150°C, g = 1mm)$. The solid line corresponds to the FE results and the dashed line to the equivalent linearized stiffness model.

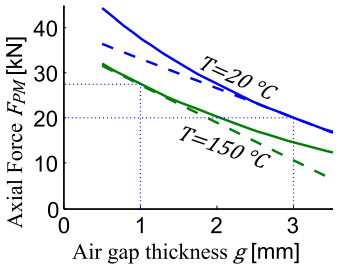

Figure 4. Linearization of the axial force in the PMTB at the airgap thickness/temperature of $(g = 3mm, T = 20°C)$ and $(g = 2\ mm, T = 150°C)$. Solid line: axial force from FEM F_{PM}, dashed line: the linearized axial force F'_{PM}

The equivalent stiffness is evaluated by the numerical derivation of the axial force generated by the PMTB:

$$k_{PM}(g,T) = -\left.\frac{\partial F_{PM}(z,T)}{\partial z}\right|_{z=g} \approx -\frac{F_{PM}(g+\delta_z,T) - F_{PM}(g-\delta_z,T)}{2\delta_z} \quad (4)$$

where $F_{PM}(z,T)$ is the axial force evaluated by the 2D axisymmetric FEM.

The equivalent natural length is obtained by:

$$z_{0,PM}(g,T) = g + \frac{F_{PM}(g,T)}{k_{PM}(g,T)} \quad (5)$$

Finally (3), (4) and (5) are summarized in:

$$\left(F_{PM}, k_{PM}, z_{0,PM}\right) = f(g,T) \quad (6)$$

Based on the equivalent linearized stiffness model, the equilibrium of the system from Fig. 3 is calculated. Using theory of series and parallel springs (see Appendix), the axial position z_1 and z_2 are obtained:

$$z_1 = \frac{k_{MB}z_{0,MB} + k_{ser}z_{0,ser}}{k_{MB}+k_{ser}} - \frac{F}{k_{MB}+k_{ser}}$$
$$z_2 = \frac{k_{PM}}{k_{PM}+k_s}z_1 - \frac{k_{PM}z_{0,PM} - k_s z_{0,s}}{k_{PM}+k_s} \quad (7)$$

with k_{ser} and $z_{0,ser}$ the equivalent stiffness and natural length of the PMTB and soft spring in series:

$$k_{ser} = \frac{k_{PM}k_s}{k_{PM}+k_s}$$
$$z_{0,ser} = z_{0,PM} + z_{0,s}$$

Solving the system of 2 equations (7) and 2 unknown variables (z_1 and z_2) at reference temperature T_{ref} gives:

- the reference position $z_{1,ref}$ and $z_{2,ref}$;
- the reference airgap thickness g_{ref};
- the reference magnetic $F_{PM,ref}$ and mechanical $F_{MB,ref}$ forces.

With a variation of temperature, i.e. $T \neq T_{ref}$, the behaviour of PMTB change. Due to the non-linearity, an iterative method has to be used. At the "start", the new magnetic force is evaluated for the same axial position but for a different temperature. In the "while loop", the following steps are implemented:

1. Evaluation of the new axial positions z_1 and z_2.
2. Evaluation of the new airgap thickness g.
3. Evaluation of the new magnetic and mechanical forces.

The sum of the two forces $F_{PM} + F_{MB}$ is compared with the total axial load F_{tot}. The convergence is reached if the error is lower than 0.01%. At the "end", the new equilibrium is calculated the new magnetic and mechanical forces, airgap thickness and axial positions are obtained. The algorithm is depicted in Fig. 5.

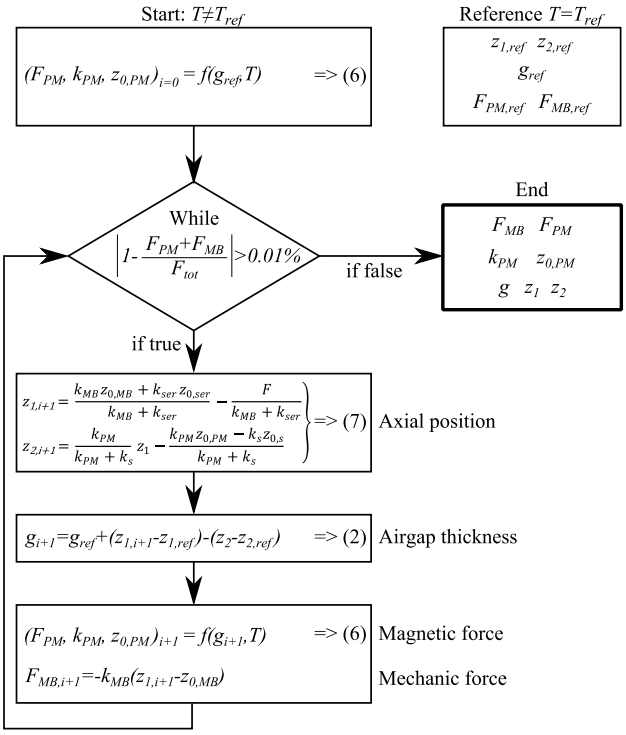

Figure 5. Algorithm used to evaluate the new equilibrium in the system. Due to the non-linearity of the axial force in the PMTB, an iterative method is used.

V. DISCUSSION

This section discusses the impact of the soft springs on the system. For the application case, the PMTB is the same as presented in section 3. The total axial load is $F_{tot} = 25\ kN$ and is distributed between the mechanical $F_{MB,ref} = 5\ kN$ and magnetic bearing $F_{PM,ref} = 20\ kN$. At room temperature (20°C), the equivalent stiffness of the PMTB is equal to $k_{PM,ref} = 6.52\ kN/mm$. The stiffness of the mechanical bearing is classically of a greater order. In a first study, it is considered to be one thousand times the PMTB stiffness: $k_{MB} = 1000\ k_{PM,ref}$. The influence of the soft springs stiffness k_s is given in relative values in comparison with the reference PMTB stiffness $k_{PM,ref}$.

In Fig. 6, the evolution of the force generated by the PMTB (a) and the equivalent airgap thickness (b) with the temperature is given for different relative soft spring stiffnesses $\frac{k_s}{k_{PM,ref}}$. Two extreme cases are presented:

- For $\frac{k_s}{k_{PM,ref}} = 10^5$, the system is strongly rigid and therefore has a behavior similar to the system without soft spring. The axial force drops with the temperature and the airgap thickness remains approximatively constant. Before irreversible demagnetization effect, the axial force is at 72% of its reference value for a temperature of $160\ ^\circ C$.
- For $\frac{k_s}{k_{PM,ref}} = 10^{-5}$, the system is strongly soft. The axial force is perfectly compensated and stays quasi-constant with the temperature. The airgap thickness is passively adapted. As observed, the axial force remains

quasi-constant even if the temperature exceeds the maximal temperature $T_{max} = 152\ ^{\circ}\ C$ (see section 3). In this region, the airgap thickness drops drastically because of the PM irreversible demagnetization.

In between these extreme cases, the soft spring acts to compensate partially the temperature effect on the magnetic force. For instance, with a soft spring stiffness equal to the reference stiffness $\frac{k_s}{k_{PM,ref}} = 1$, the axial force drops at 84% before irreversible demagnetization of $T = 158°C$. With a soft spring stiffness ten times smaller than the reference stiffness $\frac{k_s}{k_{PM,ref}} = 10^{-1}$, the axial force drops at 97% for a temperature before irreversible demagnetization of $156°C$. These values are summarized in Table II.

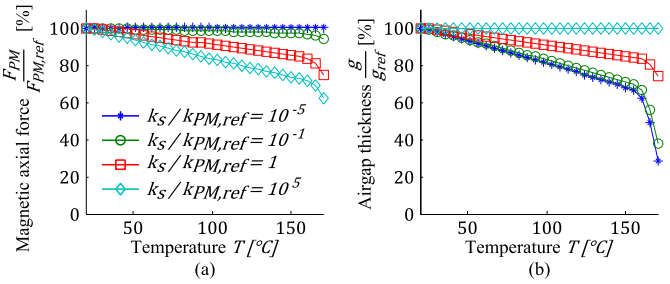

Figure 6. (a) Evolution of the magnetic axial force and (b) airgap thickness in pourcentage with the temperature for different soft spring stiffnesses.

The different curves represented in Fig. 6 show only the first increase of temperature. The hysteresis effect that could be due to an irreversible demagnetization is not taken into consideration. In case of an irreversible demagnetization occurred, the soft spring is still able to maintain a quasi-constant magnetic force even if the temperature decrease. In that case, however, the airgap thickness would not come back to its reference values but to a smaller value depending on the depth of the irreversible demagnetization.

TABLE II. EVOLUTION OF THE MAGNETIC AXIAL FORCE F_{PM} AND THE CORRESPONDING AIRGAP THICKNESS g AT THE MAXIMAL TEMPERATURE BEFORE IRREVERSIBLE DEMAGNETIZATION FOR DIFFERENT SOFT SPRING STIFFNESSES

$\frac{k_s}{k_{PM,ref}}$ [−]	$\frac{F_{PM}}{F_{PM,ref}}$	$\frac{g}{g_{ref}}$	Temperature before irreversible demagnetization
10^5	72 %	100 %	160 °C
1	84 %	83 %	158 °C
10^{-1}	97 %	69 %	156 °C
10^{-5}	100 %	67 %	152 °C

In Fig. 7.a, the evolution of the axial force with the relative soft spring stiffness is given for four different temperatures: $50°C$, $100°C$ and $150°C$ in the reversible region and $170°C$ in the irreversible region. Figure 7.b. shows the corresponding airgap thickness. We observe that for $\frac{k_s}{k_{PM,ref}}$ higher than 10, the soft spring does not compensate the temperature effect. In opposition, with a stiffness ratio $\frac{k_s}{k_{PM,ref}}$ lower than 10^{-1}, the temperature effect is well compensated.

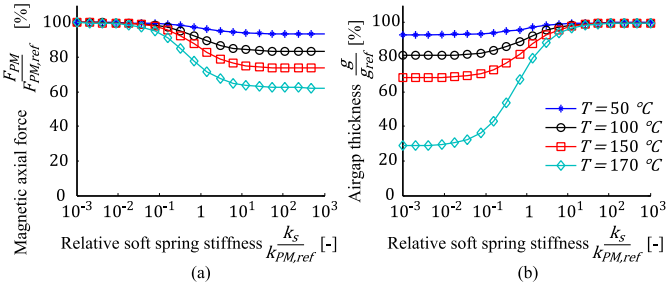

Figure 7. (a) Evolution of the magnetic axial force and (b) airgap thickness in pourcentage with the relative soft spring thicknes for 4 different temperatures: $50°C$, $100°C$ and $150°C$ in the reversible region and $170°C$ in the reversible region.

Figure 8 reveals the influence of the mechanical bearing stiffness on the global system. As explained, it is classicaly of a greater order than magnetic bearings but in some cases this difference could be smaller. Figure 8 shows the influence of the soft spring stiffness on the magnetic force (a) and airgap thickness (b) for 5 different values of mechanical stiffnesses. We observe that having a small mechanical stiffness in comparison to the magnetic stiffness helps to maintain a quasi-constant magnetic force.

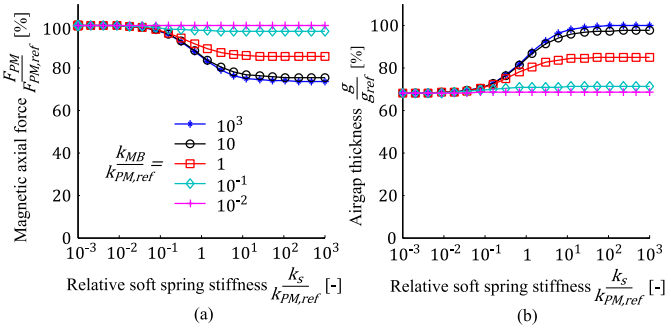

Figure 8. Evolution of (a) the magnetic axial force and (b) the airgap thickness in pourcentage with the relative soft spring thicknes for 5 different mechanical bearing stiffnesses.

VI. PRACTICAL IMPLEMENTATION

As highlighted in the previous section, in order to effectively compensate the impact of the temperature or aging, the soft spring must have a low axial stiffness in comparison to the one of the PMTB. In addition, because it is in series with the PMTB, it has to bear high axial loads. As a result of these two requirements, the soft spring must also have a long natural length.

Classical wire springs cannot meet all these requirements, at least with a reasonable footprint. However, an interesting solution could consist in using pressurized bellows as illustrated in Fig. 9. This implementation is really compact as it allows for an equivalent long natural length just by pressurizing air into the metallic bellows.

The force developed by this kind of air spring is the sum of two components, the one resulting from the action of the pressurized air F_{air} and the one due to the elastic deformation of the bellows F_{bel}. Both of them can be modeled through the Hooke's law:

$$F_{air} = -k_{air}(z - z_{0,air})$$
$$F_{bel} = -k_{bel}(z - z_{0,bel}) \quad (8)$$

with k_i the equivalent stiffness and $z_{0,i}$ the equivalent natural length, the subscript i referring to air or bellow actions. While it seems a priori relevant to consider that these two parameters are constant for the bellow action, it is not for the pressurized air one. Indeed, the equivalent stiffness due to the pressurized air is essentially a volumetric stiffness k_v which given by [6]:

$$k_{air} = k_v = \frac{p_b A_e}{V_b}\frac{\partial V_b}{\partial z} \tag{9}$$

with p_b the air pressure into the bellows, A_e the effective area of the bellows and V_b the air volume. As both the pressure p_b and the volume V_b are dependent on the displacement z, it is clear that this volumetric stiffness cannot be constant, especially if the bellows are small and the impact of the temperature and the aging on the PMTB is important. However, it is possible to reduce these dependences by connecting the bellows to an air tank so as to increase the air volume V_b without impacting the size of the bellows. This therefore allows for obtaining a quasi-constant equivalent air stiffness, but also a lower value for this stiffness.

Fig. 9 illustrates different implantations of bellow-based air springs. In Fig.9.a, a pneumatic bellows is schematically represented. In that specific case, the equivalent stiffness related to the elastic deformation of the bellows k_{bel} can be neglected, as the corresponding force. In that specific case however, the equivalent stiffness of the air action k_{air} is the sum of the volumetric stiffness k_v given in (9) and the area stiffness k_a given by [6]:

$$k_a = -(p_b - p_a)\frac{\partial A_e}{\partial z} \tag{10}$$

with p_a the ambient pressure. Figures 9.b and 9.c show implementations based on pressurized metal bellows or diaphragm bellows respectively. In these cases, the stiffness linked to the bellows or to the diaphragm itself, is higher and has therefore to be considered, besides the air pressure.

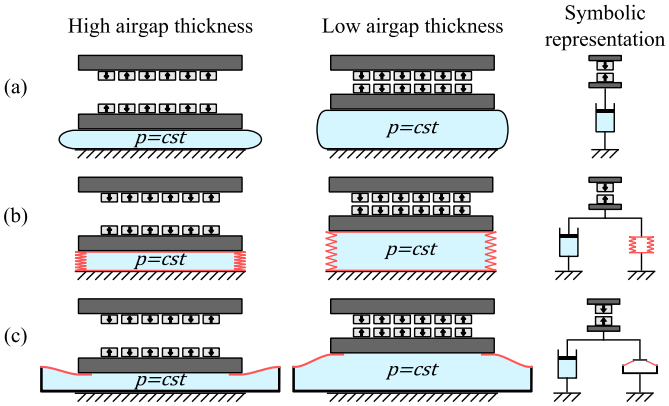

Figure 9. Pratical implementation of pressurized air-based soft spring with high load capacity. (a) The pressurized pneumatic bellows, (b) the pressurized metal bellows, (c) the pressurized diaphragme billows.

VII. CONCLUSION

Combining permanent magnet thrust bearings and mechanical bearings allows for relieving the load on the latter and therefore reducing the losses and increasing the lifetime of the system. Due to temperature effect and aging, the performance of the permanent magnet can however deteriorate. This paper shows that placing a soft spring in series with the static part of the PM bearing is a solution for maintaining a quasi-constant magnetic force. Practically, the need of low stiffness but high force means a high natural length. To implement these characteristics, soft springs based on bellows are presented.

ACKNOWLEDGEMENT

This work was supported by convention no. 6977 with the Walloon Region.

REFERENCES

[1] M. Recheis *et al.*, "Improving kinetic energy storage for vehicles through the combination of rolling element and active magnetic bearings," in *Industrial Electronics Society, IECON 2013-39th Annual Conference of the IEEE*, 2013, p. 4641–4646.

[2] C. S. Toh and S. L. Chen, "Design and control of a ring-type flywheel battery system with hybrid halbach magnetic bearings," in *Advanced Intelligent Mechatronics (AIM), 2014 IEEE/ASME International Conference on*, 2014, p. 1558–1562.

[3] J. J. Pérez-Loya, C. J. D. Abrahamsson, F. Evestedt, et U. Lundin, "Performance Tests of a Permanent Magnet Thrust Bearing for a Hydropower Synchronous Generator Test-Rig," *Applied Computational Electromagnetics Society Journal*, vol. 32, nº 8, 2017.

[4] M. Van Beneden, V. Kluyskens, and B. Dehez, "Axial force evaluation in permanent magnet thrust bearings subject to demagnetization and temperature effects," *ISMB16, Pekin, 2018*

[5] M. Van Beneden, V. Kluyskens, and B. Dehez, "Comparison between optimized topologies of permanent magnet thrust bearings with back-iron," *Mechanical Engineering Journal*, vol. 4, nº 5, p. 17-00061-17-00061, 2017.

[6] N. Docquier, P. Fisette, H. Jeanmart. "Model-based evaluation of railway pneumatic suspensions". Veh Syst Dyn. 2008, 46(S1), 481–493

APPENDIX

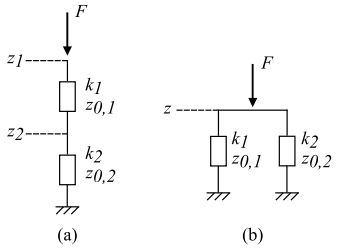

Figure 10. (a) Two series springs, (b) Two parallel springs

The equivalent model of 2 series springs (Fig. 10.a) is:

$$F = \frac{k_1 k_2}{k_1 + k_2}\left(z_1 - \left(z_{0,1} + z_{0,2}\right)\right)$$

with the position of the middle point z_2:

$$z_2 = \frac{k_1}{k_1 + k_2} z_1 - \frac{k_1 z_{0,1} - k_2 z_{0,2}}{k_1 + k_2}$$

The equivalent model of 2 parallel springs (Fig. 10.b):

$$F = -(k_1 + k_2)\left(z - \left(\frac{k_1 z_{0,1} + k_2 z_{0,2}}{k_1 + k_2}\right)\right)$$